RSC Advances

REVIEW

View Article Online
View Journal | View Issue

Cite this: *RSC Adv.*, 2025, **15**, 45359

Advances in predicting human olfactory perception: from data acquisition to computational models

Tao Zhou,[a] Jian Ma,[a] Zongwei He,[a] Chuan He,[a] Xixiang Zhang,[a] Xiao Wu,[a] Hao Li,[a] Xiaoya Xie,[b] Long Chen*[ab] and Xing Chen*[b]

Researchers endeavor to collect odor information to prepare for the exploration of odor prediction. Such researches will require machine learning algorithms with excellent data processing capabilities. Odor perception also requires advanced sensor performance, including sensitivity, selectivity, stability and minimum lower limits of detection. Gas sensing technologies play a key role in identifying gas mixtures by providing critical response signals and characterization data. Here, we explore the recent advances in gas sensing technologies to meet the pivotal needs of human olfactory perception. First, we summarize the databases of olfactory perception. Then, the fundamental sensing principles of gas chromatography-mass spectrometry and metal-oxide semiconductor, optical, and electrochemical sensors for molecular odor prediction are briefly introduced. Finally, we connect the odor-related sensing technology with suitable machine learning algorithms, encompassing areas like artificial neural networks (ANN), random forest (RF), K nearest neighbors (KNN), support vector machine (SVM), extreme learning machine (ELM), gradient boosting decision tree (GBDT), and decision tree (DT) approaches. In the future, machine learning is expected to help build an understanding of the link between odors and human olfactory sensory mechanisms, consequently making a significant contribution to olfactory research.

Received 15th September 2025
Accepted 7th October 2025

DOI: 10.1039/d5ra06959a

rsc.li/rsc-advances

1. Introduction

Olfaction, as a critical sensory modality for environmental perception, conveys rich chemical information—from natural fragrances to hazardous volatiles—profoundly influencing animal behavior and emotional states.[1]

For humans, olfactory perception is a complex chemosensory process that begins in the nasal cavity and culminates in the brain. Its fundamental principle is that volatile organic compounds (VOCs) combine to specific olfactory receptors, triggering neural signals.[2] These signals are relayed and processed, ultimately being recognized by the cerebral cortex and interpreted as a conscious perception of smell.

The working mechanism of olfaction can be broken down into the following key steps: (1) odorant inhalation and transport, during which airborne molecules are conveyed to the olfactory epithelium and dissolve in the mucosal layer; (2) olfactory receptor activation, where odorants interact with one of the approximately 400 types of G protein-coupled receptors located on the cilia of the olfactory sensory neurons; (3) signal transduction and impulse generation, mediated by a cAMP-dependent pathway that elicits neuronal depolarization and action potential propagation; (4) neural convergence and integration, achieved *via* the projection of olfactory neuron axons onto glomerular units within the olfactory bulb, facilitating initial odorant mapping; and (5) central processing and perception, wherein olfactory information is relayed by mitral cells to a distributed cortical network, including the piriform cortex, amygdala, and entorhinal cortex, resulting in odor identification, memory association, and emotional valuation[3,4] (as shown in Fig. 1). Studies suggest the human nose can discriminate up to a trillion olfactory stimuli,[5] with distinct molecular features eliciting divergent hedonic responses (*e.g.*, pleasant aromas *vs.* putrid odors). While conventional odor analysis relies on labor-intensive techniques (*e.g.*, gas chromatography-mass spectrometry, GC-MS, and electronic nose[6]) or subjective panels, these methods lack scalability for real-time, complex odor profiling. This is primarily because the complexity of odorant–receptor interactions and the dynamic nature of real-world odor mixtures pose significant challenges for traditional analysis methods. To address these limitations, emerging bionic and AI-driven approaches offer transformative solutions. For instance, electronic noses and tactile-olfactory fusion systems (*e.g.*, star-nose-inspired bionic arrays) enable robust odor discrimination and object recognition in non-visual environments by mimicking multisensory biological perception. Machine learning further augments these platforms by

[a]*China Tobacco Sichuan Industrial Co., Ltd, Chengdu 610101, China. E-mail: senlongchen@zju.edu.cn; cnxingchen@zju.edu.cn*
[b]*Biosensor National Special Laboratory Department of Biomedical Engineering, Zhejiang University, Hangzhou 310027, China*

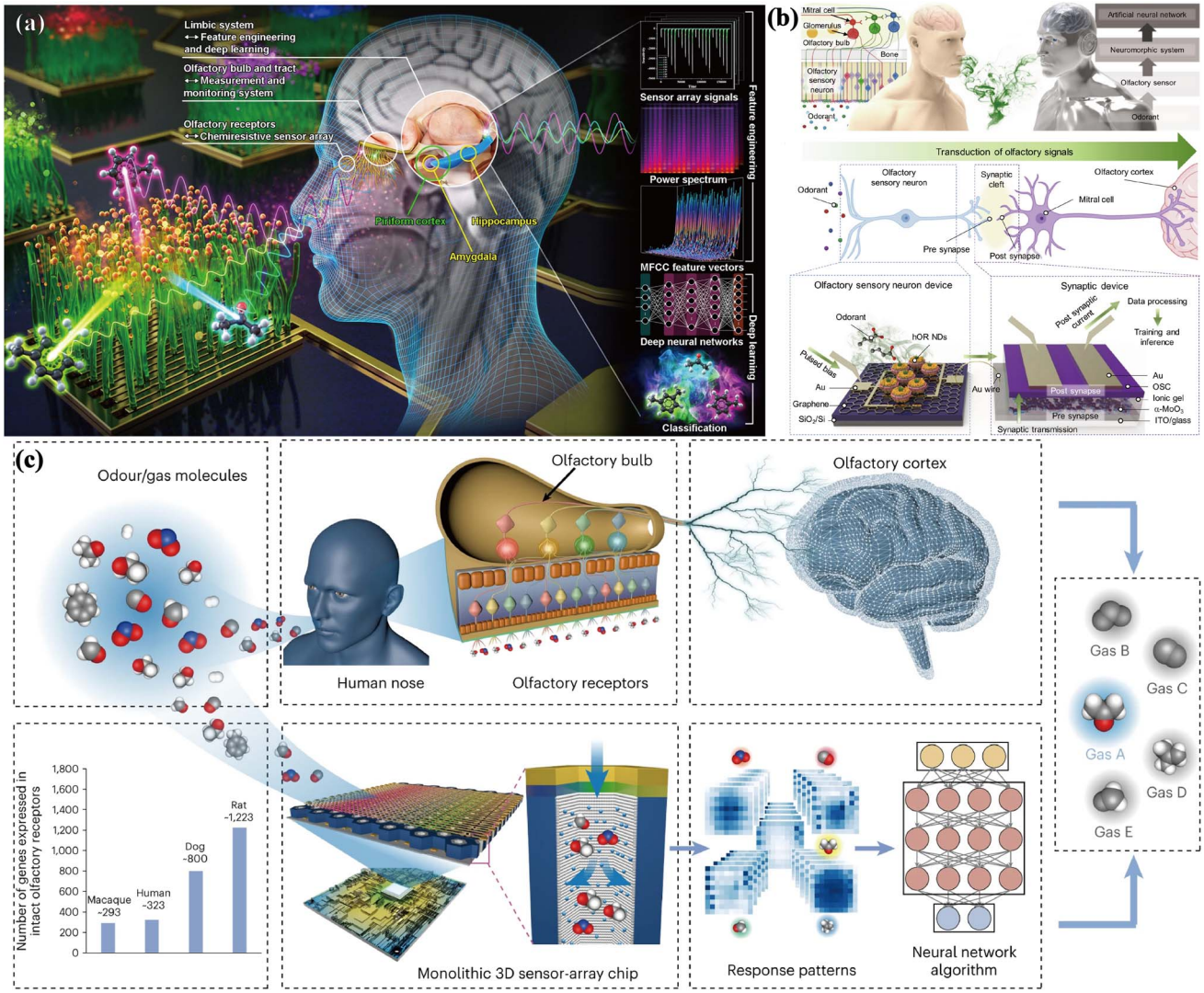

Fig. 1 Schematic of the pathway of the biomimetic olfactory system. (a) Reproduced with permission.[7] Copyright from Springer Nature, 2024. (b) Reproduced with permission.[8] Copyright from AAAS, 2024. (c) Reproduced with permission.[9] Copyright from Springer Nature, 2024.

extracting latent structure–odor relationships from large datasets, enabling predictive modeling of unknown odorants based on molecular features. In another study, a data-centric artificial olfactory system is described that addresses the limitations of conventional sensitivity-oriented approaches by introducing an Eigengraph-based electrochemical analysis. By mathematically encoding implicit odor attributes as Mel-Frequency Cepstral Coefficient (MFCC) feature vectors *via* the Fourier transform, their method enables deep learning-driven in-depth analysis of gas molecules. Experimental validation on mixed gases and automotive exhaust demonstrates its effectiveness in gas classification. This work establishes a foundation for standardized artificial olfactory systems, offering a scalable framework for advancing electronic nose technology.[7]

The human olfactory system demonstrates remarkable discriminative capability because it contains a diverse array of receptor cells that selectively respond to specific gas molecules. For a long time, the replication of such biological complexity in artificial olfactory systems has been hindered by a fundamental challenge: the high-performance monolithic integration of large-scale, heterogeneous sensor arrays. However, innovations in nanomaterials and system integration technology are gradually addressing this limitation. For instance, Wang *et al.* demonstrated a bio-inspired olfactory chip that was integrated with 10 000 individually addressable nanotube sensors on a nanoporous substrate. When coupled with artificial intelligence, this platform achieves exceptional sensitivity and discriminative capacity—successfully identifying 24 distinct odors and complex gas mixtures. Furthermore, its integration with vision sensors in a robotic dog system highlights its potential for multimodal sensing in real-world applications.[9] This shift, from manual analysis to automated, data-driven odor characterization models, enables high-throughput, objective odor assessment across applications ranging from environmental monitoring to biomedical diagnostics. Machine learning can realize the prediction and classification of unknown data by learning a large amount of data sets and discovering the hidden rules in the data.[10] In the domain of

odor research, machine learning can realize the objective description and odor prediction by analyzing the structural information of odor molecules and building a prediction model.[11] Despite these advances, the practical implementation of machine learning in odor prediction still faces challenges, particularly in achieving generalizability across diverse sensing data and perceptual descriptors. To bridge this gap, recent studies have focused on developing more robust and interpretable models that are capable of capturing the nonlinear relationships between sensing data and human olfactory perception. Such models not only require large-scale, high-quality datasets but also sophisticated algorithms to handle the complexity of odorant–odor associations.

This review systematically summarizes the recent advancements and practical applications of olfactory perception prediction models from sensing data, based on machine learning (as shown in Fig. 2). The article first introduces typical sensing devices. Subsequently, it outlines the application cases and experimental results of machine learning for odor prediction in recent years, presenting key findings and analyzing both advantages and limitations. Finally, the article concludes by exploring prospective developments and potential applications of machine learning in odor prediction through advanced sensing technologies.

2. Database of olfactory perception

2.1 The odorant database and olfactory perception

The growth of large models and big data is accelerating advancements in science and technology. Olfactory datasets play an important role in simulating the human sense of smell, odor identification, environmental monitoring, health monitoring, and robotics.[12] For example, Schreurs *et al.* described the olfactory space and found that 40 billion possible compounds are odorous.[13] In order to understand the smell of a substance, Keller *et al.* presented volunteers with a panel of odorants and asked them to evaluate the perceptual qualities of each.[14] They established an olfactory psychophysical dataset that included geometrical and topological properties, functional groups, and atom types. Chacko *et al.* developed another odor database comprising 480 distinct substances linked to approximately 55 000 associated perceptual responses. For each molecule, they provided detailed perceptual ratings across three key dimensions: odor intensity, pleasantness, and familiarity. Gamboa *et al.* developed a comprehensive time-series dataset utilizing a metal oxide semiconductor (MOS) gas sensor array to evaluate the spoilage thresholds in wines, offering significant insights into food quality monitoring. This dataset, which is publicly accessible, has been deposited in an open repository at **https://data.mendeley.com/datasets/vpc887d53s/**, facilitating broader research collaboration and reproducibility in the field of food science. The innovative approach underscores the potential of sensor-based technologies to enhance food safety and shelf-life assessment.[15] Similarly, the e-nose dataset for meat was used to analyze the quality of beef, as well as to discriminate between beef and pork.[16,17] Electronic nose (e-nose) sensor arrays classify and quantify gases but suffer from measurement drift over time due to chemosensory response changes, compromising long-term data reliability. To enhance gas quantification accuracy, Gordillo *et al.* developed a regression approach that integrates machine learning techniques with domain adaptation using the Kullback–Leibler importance estimation procedure (KLIEP).

They trained and tested their model on a three-year dataset from a 16-sensor e-nose array to validate its accuracy and robustness.[18] QuantumScents introduces a quantum mechanics-enhanced derivative of the Leffingwell data set, featuring 3.5 k diverse molecules (2–30 heavy atoms) with 3D

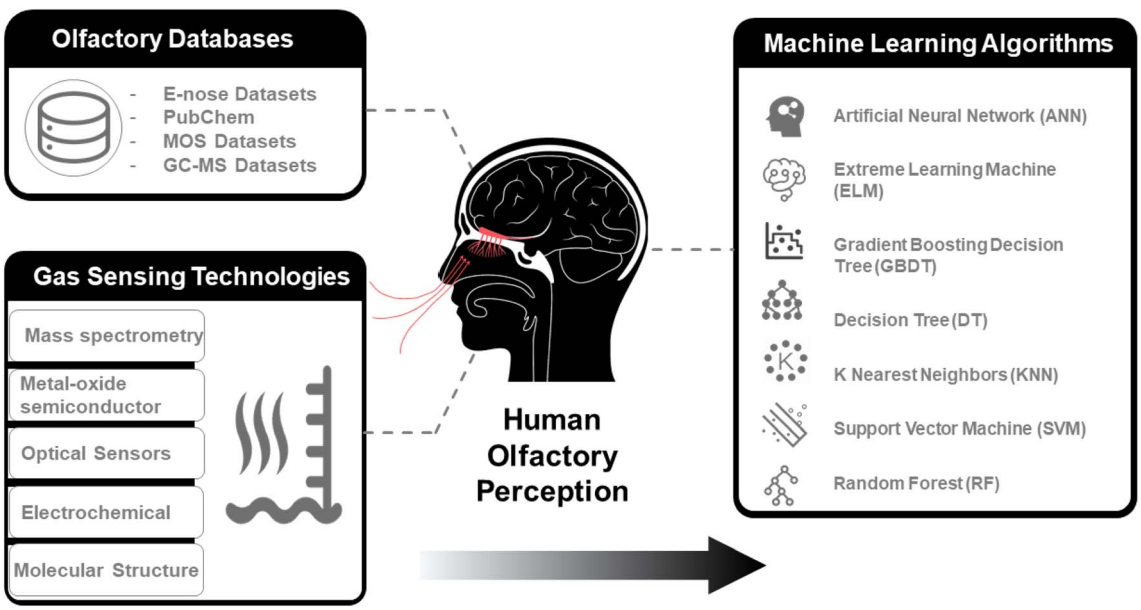

Fig. 2 Human olfactory perception.

coordinates, PBE0 energy, dipole moments, and Hirshfeld charges. Burns *et al.* demonstrated the utility of Hirshfeld charges for molecular scent classification using a message passing neural network. The dataset and related resources are freely accessible on Zenodo (**https://zenodo.org/doi/10.5281/zenodo.8239853**).[19]

PubChem, established in 2004 under the National Institutes of Health (NIH) Molecular Libraries Roadmap Initiatives, has evolved into a pivotal chemical information repository for the scientific community. It encompasses three interconnected databases: substance, compound, and BioAssay, which collectively provide comprehensive data on chemical substances, their unique structures, SMILES, CID, chemical properties, and biological activities. Another study delineated the architecture and functionalities of the substance and compound databases, detailing data sources, organization, submission protocols, chemical structure standardization, and search interfaces. Additionally, it introduces PubChem3D, offering theoretical 3D structures of compounds, and PubChemRDF, facilitating data sharing and integration through RDF-formatted resources.[20]

Nevertheless, comprehensive odor databases, integrating both chemical concentration profiles and corresponding olfactory analysis results, remain notably absent in the current literature. A preliminary database framework of multi-source measurement data will be meaningful. The above database is anticipated to provide an online platform for storing, sharing, retrieving, updating, and mining odor perceptional data. It is expected to make a website available; thus, workers, researchers, and research institutions in the area of olfactory studies could register, upload and analyze data to help enrich the multi-source measurement database. Researchers can also download and retrieve relevant data from the website within certain limits of authority. Besides inputting data manually, artificial intelligence algorithms can be used to extract, calculate and analyze data through the database. Odor measurement data shows source characteristics, and each olfactory data point can include mass spectrometry, MOS measurement, electrochemical, and optical sensor data, as well as data from molecular structure and olfaction. Multiple measurement data sources can uncover information about the substance in multiple dimensions. Meanwhile, users can search the data based on olfactory characteristics, such as the odorous and odorless, or by inputting keywords into the search options.

2.2 The algorithm between an odorant database and olfactory perception

Databases and algorithms maintain a symbiotic relationship in data-driven research, where databases provide organized data storage and retrieval mechanisms, while algorithms enable systematic data processing, pattern recognition, and knowledge extraction through computational operations. Specifically, advanced algorithmic approaches play a crucial role in uncovering latent patterns and correlations within complex datasets. Algorithms can mine the potential value of data and better understand the relationships between substances and olfactory data. The algorithms utilized for olfactory analysis encompass artificial neural networks (ANN), random forests (RF), K-nearest neighbors (KNN), support vector machines (SVM), extreme learning machines (ELM), gradient boosting decision trees (GBDT), decision trees (DT), and principal components analysis (PCA). The performance of artificial neural network algorithms in olfactory analysis demonstrates a positive correlation with dataset size, as larger datasets significantly enhance the model's analytical capabilities. Furthermore, ANN operates as a black-box model with limited interpretability, and RF is a white box. In other words, the RF is more interpretable than ANN. Other algorithms, such as layer neural networks, deep neural networks, deep belief networks, gradient boosting machine, LightGBM, and adaptive boosting k-nearest neighbors, have been constructed to predict odor perception.

3. Odor impression prediction research

In recent years, odor impression prediction (*e.g.*, pleasantness, intensity, and familiarity) has become a hot topic in olfactory research. The relevant research methods can be categorized into three broad groups: mass spectrometry, electronic nose (e-nose), and molecular characterization.

3.1 Mass spectrometry

In numerous studies, gas chromatography-mass spectrometry is typically used to detect and quantify volatile organic compounds (VOCs). The test sample is added to the inlet through an injection tank and then passed through a capillary column with the help of carrier gas, usually an inert gas. At the column outlet, VOCs in the sample are ionized, passed through an electromagnetic field, and filtered by mass-to-charge ratio. The mass spectrometer ultimately analyzes the mass-to-charge ratio to provide a fingerprint of the sample. As one of the most common analytical techniques, Gas Chromatography-Mass Spectrometry (GC-MS) is the gold standard for VOCs analysis. To address the limitations of GC-MS, researchers have developed various advanced analytical platforms, such as selective ion flow tube-mass spectrometry (SIFT-MS), ion mobility spectrometry (IMS), solid-phase microextraction/gas chromatography-mass spectrometry (SPME/GC-MS), and proton-transfer reaction-mass spectrometry (PRT-MS).

When the concentration of volatile organic compounds is at the parts per billion level, the identification of VOCs is typically achieved by gas chromatography-mass spectrometry (GC-MS). For example, a recent study measured 19 odorants in wine using GC-MS, and built a relationship between the odorants' concentrations with an electronic nose.[21] Another investigation of VOCs using GC-MS was conducted to analyze the influence of ageing method and ageing time on roast beef tenderloin.[22] Significant differences in biomarker profiles were observed between wet-aged and dry-aged beef, with notably higher concentrations of alkyl-pyrazines, 3-hydroxy-2-butanone, and 2-acetyl-2-thiazoline detected in dry-aged samples compared to their wet-aged counterparts. Other types of VOCs have also been explored using GC-MS. For instance, a study used GC-MS for

classifying gluten and non-gluten cereal flour,[23] constructing a model that achieved an impressive 85.71% accuracy in distinguishing botanical origins. In a separate investigation, the aromatic profile of wine was systematically analyzed utilizing GC-MS. This study represents the first documented identification of ethyl formate, methyl acetate, and amyl acetate as constituent compounds in Sauvignon Blanc wine.[24] Meanwhile, the authors used artificial neural networks (ANN) to model wine aroma and sensory quality, and the accuracy of the model was 95.4%. Similarly, gas chromatography was used to analyze Wuyi rock tea, and the multilayer perceptron obtained an average accuracy of 92.7% from 330 tea samples.[25] In another study, conducted by Chen *et al.*, an experiment was designed to investigate freshness biomarkers in fish. The researchers utilized a Random Forest algorithm to analyze the correlation between sensory fish odor and long-chain polyunsaturated fatty acids. The model revealed that specific chemical classes, including aldehydes, ketones, alcohols, and furans, were significantly associated with the perception of fishiness. These findings provide valuable insights into the chemical basis of odor-related freshness indicators in fish.[26]

3.2 Electronic nose

Electronic nose (E-nose) systems are an array of gas sensors. They are fundamentally inspired by the human nose and are designed to identify, recognize, and analyze volatile organic compounds or gas biomarkers in various environments. An electronic nose prototype can be classified into metal oxide semiconductor, optical sensor, and electrochemical systems.

3.2.1 Metal-oxide semiconductors. Resistive metal oxide semiconductor (MOS) sensors are the most widely used gas sensors.[27] As shown in Fig. 3(a), current electronic noses are not yet comparable to the human nose,[28] but researchers are using large arrays of sensors to mimic human olfaction as closely as possible. The structure of this MOS gas sensor is coated with a metal oxide gas-sensitive thin film on its surface, which is used to adsorb and detect target gases (Fig. 3(b)).[29]

The sensitizing material of the MOS is commonly an n-type semiconductor, such as ZnO, SnO_2, In_2O_3, TiO_2, Fe_2O_3 or WO_3.[30] Zinc oxide (ZnO) is regarded as an ideal material for making gas sensors because of its high electron mobility, photoelectric response, wide bandgap, and excellent thermal and chemical stability. As shown in Table 1, oxygen molecules in the air adsorb electrons from the conduction band and form different ionized oxygen (O^- 2, O^-, and O^{2-}) at different working temperatures. The relevant reactions can be expressed as follows:

The process of developing ionized oxygen can generate an electron depletion layer (EDL) near the surface of the MOS. A broad EDL in the MOS will form a sensitive material in a highly resistive state. Upon reducing the gas, the adsorbed electrons transfer from the gas to the MOS, and the thickness of the EDL becomes narrow, leading to a low-resistance sensor. The p-type MOS reacts with gases in the opposite way to the n-type. The change in resistance between the two gases is the detection signal of the MOS electronic nose.

MOS gas sensors are mainly noble-metal-decorated MOS, metal-ion-doped MOS, and composite MOS (as shown in Table 2). According to Yang's report,[35] noble metal (Au, Pt) decorated WO_3 exhibited an excellent response to methyl salicylate with a low limit of detection (100 ppb) compared to pure WO_3 nanofibers. The sensor also showed an excellent response when using metal-ion-doped MOS. For example, Co-doped In_2O_3 displayed an exceptional response toward triethylamine with an obvious response of 3500.[36] Sensors using composite MOS can construct heterojunctions, thereby accelerating the transport of electrons at the interface and ultimately altering the thickness of the EDL at the surface of the MOS. For example, a sensor based on a MoS_2/TiO_2 composite displayed a selective response to ethanol and methanol at the ppm level. Furthermore, the sensor also exhibited long-term stability and anti-humidity resistance in the range of 20% to 90%.[37]

Studies have revealed that different nanostructured shapes (*e.g.*, nanoparticles, nano-thinfilms, nanotubes, nanoflowers, nanosheets, nanowires, nanorods, and nanofibers) have a high

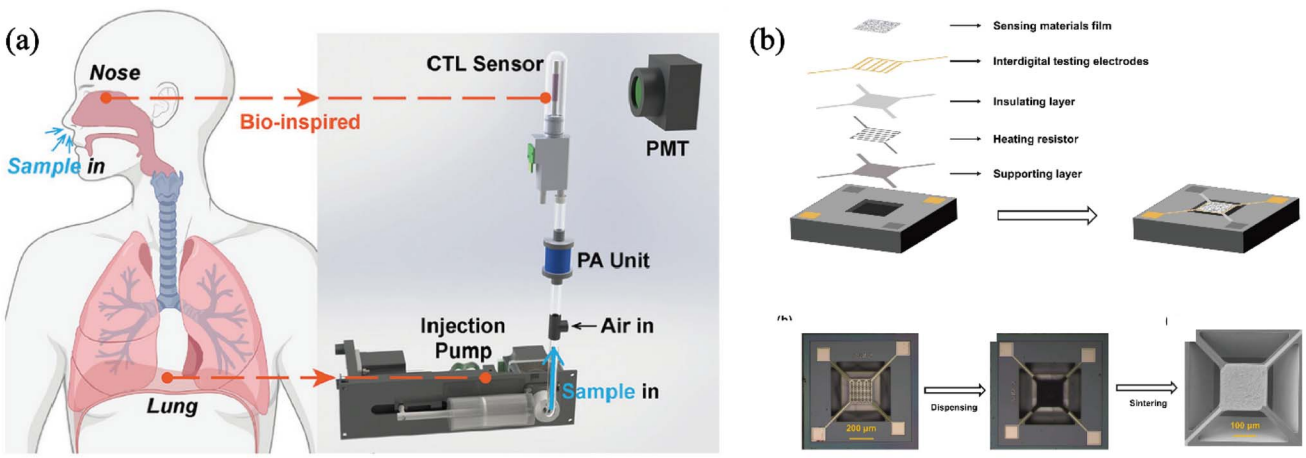

Fig. 3 (a) Sensor array used as an electronic nose. Reproduced with permission.[28] Copyright from Wiley, 2024. (b) Schematic of a common MOS framework. Reproduced with permission.[29] Copyright from MDPI, 2025.

Table 1 Reaction processes on an MOS gas sensor

Analytes	Reaction process	Temperature	Ref.
Ionized oxygen	O (gas) ↔ O_2 (ads)	RT	31
	O_2 (ads) + e^- ↔ O_2^- (ads)	T < 100 °C	32
	O_2^- (ads) + e^- ↔ $2O^-$ (ads)	100 °C < T < 300 °C	33
	O^- (ads) + e^- ↔ O^{2-} (ads)	T > 300 °C	34

Table 2 Brief summary of MOS gas sensors

Material	Target gas	Opt (°C)	T_{res}	T_{rec}	Synthesis method	Con (ppm)	Res	Ref.
Ag/ZnO	Ethanol	325	NA	NA	Sol–gel	50	32.5	38
Eu/SnO_2	Acetone	280	4	3	Electrospinning	100	32.2	39
Ni/ZnO	H_2S	215	50	124	Electrospinning	50	474	40
Mo/SnO_2	Ethanol	220	7	103	Electrospinning	100	46.8	41
Co/ZnO	Acetone	370	60	77	Hydrothermal	5	18.5	42
Cr/ZnO	Ethanol	300	NA	NA	Hydrothermal	400	45	43
Dy/In_2O_3	Ethanol	250	5	248	Hydrothermal	100	85	43

surface-to-volume ratios, which indicate that gases are easily diffused from the surface of the material (as shown in Fig. 4). Suitable nanostructures contribute to the design of high-performance gas sensors. Characteristic gaseous biomarkers are produced when food spoils during production and transportation. Therefore, the assessment of food freshness is important for food quality and safety. For example, a $SnSe_2$/WO_3-composite-based gas sensor was designed to evaluate egg spoilage at room temperature.[48] The sensor demonstrated a response value of 33.8% toward 10 ppm of H_2S. In another work, the Pd-decorated ZnO was prepared using a simple wet chemical method. The sensor detected meat spoilage by monitoring 400 ppm methyl amine with a response value of 99.5%.[49]

The morphology, limit of detection (LOD), response/recovery time, and optimal working temperature are all significant aspects of sensing performance. These factors provide

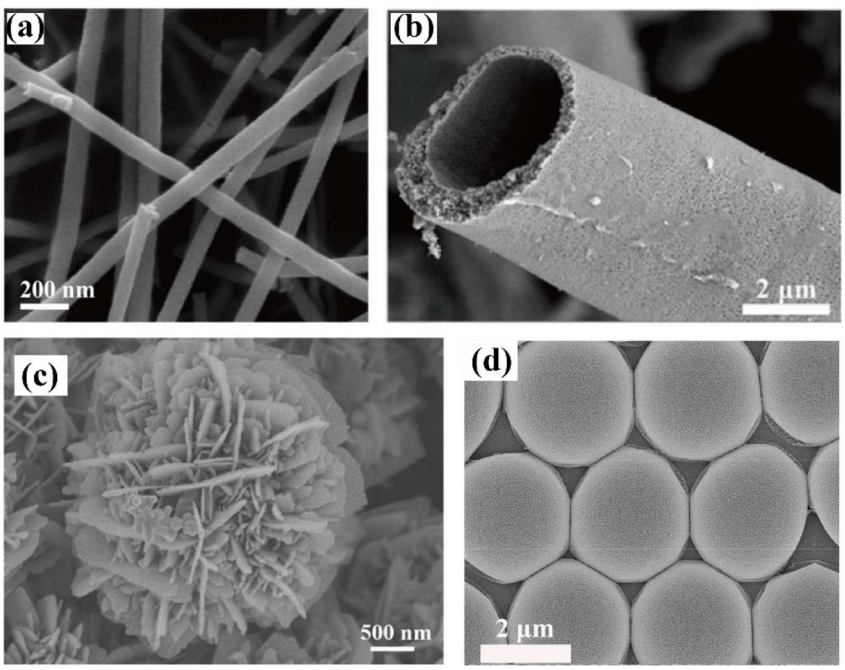

Fig. 4 (a) Scanning electron microscopy images of nanofibers. Reproduced with permission.[44] Copyright from Elsevier, 2024. (b) Scanning electron microscopy images of nanotubes. Reproduced with permission.[45] Copyright from Elsevier, 2023. (c) Scanning electron microscopy images of nanoflowers reproduced with permission.[46] Copyright from Elsevier, 2024. (d) Scanning electron microscopy images of nanospheres. Reproduced with permission.[47] Copyright from Elsevier, 2024.

a comprehensive summary of the characteristics of MOS gas sensors.

3.2.2 Optical gas sensors. Optical gas sensors utilize the interaction between light and target gas molecules to detect and quantify gas concentrations. Compared to traditional electrochemical or MOS sensors, they generally offer higher selectivity, sensitivity, faster response times, and greater resistance to poisoning or aging, making them widely applicable in various fields. The basic principle of all optical gas sensors is based on optical phenomena that occur when light interacts with matter. When a beam of light passes through a gas, the gas molecules change the light's absorption,[54] fluorescence,[55] scattering,[56] and refractive index[57] in specific ways, and these changes are mapped to the concentration of the gas (as shown in Fig. 5(a)). Optical sensors exhibit better selectivity for gas detection and can work at ambient temperature conditions. For instance, Wang *et al.* developed a ZIF-67-based sensor that demonstrated remarkable selectivity for 2-chloroethyl ethyl sulfide (CEES) detection, effectively distinguishing it from seven potential interfering gases[51] (as shown in Fig. 5(b)). Most importantly, the optical gas sensor has excellent moisture resistance, ultrafast response (0.5 s), long-term stability and reusability, and an ultralow detection limit (19.1 ppb) for CEES at 95% RH. As shown in Fig. 5(c), the test gas concentration can be determined by its infrared absorption characteristics utilizing non-dispersive infrared spectroscopy (NDIR). The NDIR sensor with nanoantenna integrated narrowband detectors can detect the gases of H_2S, CO_2, CH_4, NO, CO, SO_2, NO_2, and CH_2O.[52] Meanwhile, the NDIR can also recognize gases in a mixture and exhibit an ultralow detection limit toward CH_4 (63 ppm), CO_2 (2 ppm), and CO (11 ppm). By combining metal elements with light-emitting diodes, a ChemLED array was successfully fabricated. The fabricated device, comprising 100 distinct ChemLED units, demonstrated responsive characteristics toward gas mixtures, enabling the artificial olfactory system to accurately predict both the gas concentrations and chemical compositions.[50] In a similar manner to MOS noses, colorimetric sensors can mimic human olfaction. The mechanisms of colorimetric sensor arrays can provide color changes when the sensor array responds to analyte types, and the color difference maps can typically provide lower limits of detection, at the ppb level[53] (as shown in Fig. 5(d)). The odor visualization was also applied to freshness monitoring. For example, ammonium quaternized cellulose nanofibers (C-CNFs) were designed to recognize volatile organic compounds (VOCs) at 60% RH. The C-CNFs exhibited a low detection limit for ammonia (2 ppm), trimethylamine (3 ppm), dimethylamine (21 ppm), putrescine (1 ppm), and cadaverine (1 ppm). The integration of colorimetric sensor arrays with convolutional neural network (CNN) technology enables the detection of key freshness biomarkers, including ammonia, trimethylamine, dimethylamine, putrescine, and cadaverine. This combined analytical model demonstrates exceptional performance in freshness monitoring, achieving a high predictive accuracy of 99%.[58] In order to meet natural olfaction features, one study bridges the gap between artificial and biological olfaction by employing a biologically inspired processing algorithm applied to a highly redundant sensor array. Using a webcam to capture RGB color intensities from 15 optical indicators exposed to chemical vapors, each pixel was treated as a sensor, yielding ~28 000 copies representing 45 cross-selective virtual receptors. This redundancy facilitated the modeling of the olfactory bulb as a network of inhibitory and excitatory elements, while a Self-Organizing Map (SOM) generated an over-segmented reference space to track the real-time adsorption–desorption pathways of activated neurons. The system demonstrated robust odor identification, despite 65% sensor anomalies, offering a scalable platform for implementing algorithms that mimic biological olfaction pathways.[59,60]

3.2.3 Electrochemical gas sensors. The gas-sensing principles underlying electrochemical gas sensors are based on redox reactions.[64] The reaction generates or consumes current, which is proportional to the gas concentration. As shown in Fig. 6(a), such sensors are composed of a counter, a reference, and a working electrode that are immersed in an electrolyte. Usually, a gas-permeable membrane covers the sensing electrode to control the volume of gas diffusing toward the electrode surface. Electrochemical gas sensors are primarily classified into three distinct categories according to their fundamental operating principles: potentiometric, amperometric, and conductometric sensors. Notably, the development of such sensors has been significantly influenced by biological systems, particularly in mimicking their efficiency and sensitivity. As shown in Fig. 6(b), an olfactory-inspired organic electrochemical transistor (OI-OECT) integrates chemical sensing, tunable memory, and selective gas recognition in a single device. The ion-gel electrolyte enables low-voltage operation and synaptic-like behaviors, including inhibitory postsynaptic currents and paired-pulse facilitation. The device demonstrates volatile-to-nonvolatile memory switching *via* gate voltage modulation (0 to −1 V) and functions as an early warning system for gas leaks (*e.g.*, NH_3 and H_2S) through cumulative exposure detection. This work provides a compact platform for artificial olfaction by combining signal transduction, adaptive memory, and gas discrimination.[62] Lu *et al.* reported high-performance stretchable all-gel OECTs using semiconducting polymer gel active layers and poly(ionic liquid) ionogel electrolytes. The interconnected gel network facilitates ion transport while maintaining structural integrity under strain, achieving an optimal balance between stretchability (50%) and electrical performance (transconductance: 86.4 mS, on/off ratio: 1.2×10^5). These devices demonstrate exceptional cycling stability (10 000 cycles at 30% strain) and multifunctionality as electronic skins for robotic tactile sensing, neuromorphic synapses, and gas sensors for food quality monitoring[63] (as shown in Fig. 6(c) and (d)). Inspired by the neuronal network within the olfactory bulb glomerulus, one study reported an artificial chemosensory synapse that chemically modulates neurotransmitter-like excitatory/inhibitory responses, mirroring synaptic plasticity in olfactory pathways. The device, based on a flexible organic electrochemical transistor gated by a chemoreceptive ionogel, demonstrates long-term memory retention and erasure through ion dynamics, mimicking key functions of the human olfactory system. This innovation

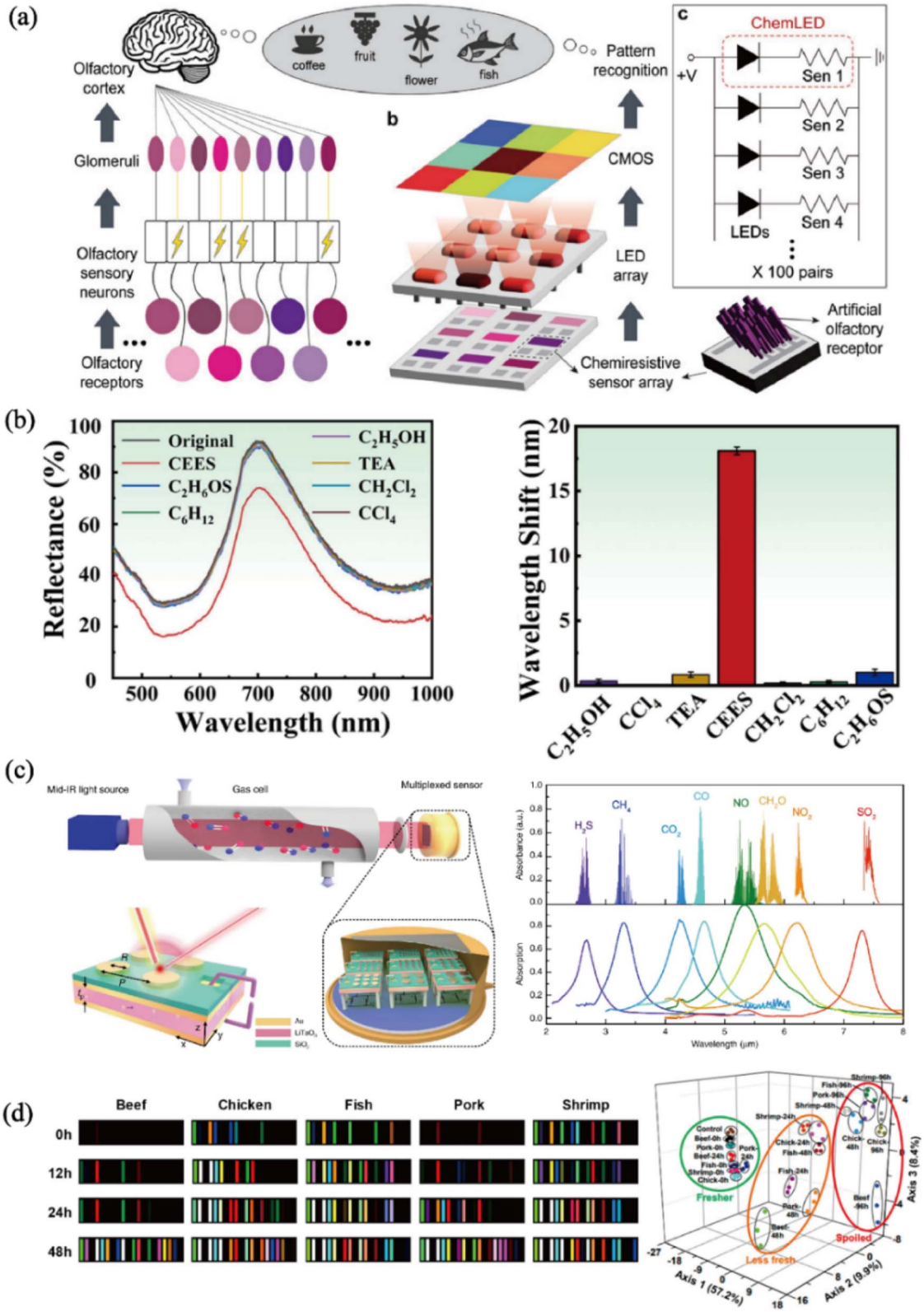

Fig. 5 (a) Biological olfaction system and ChemLED. Reproduced with permission.[50] Copyright from Wiley, 2024. (b) Sensor reflection spectra after gas exposure and the associated wavelength shift distribution. Reproduced with permission.[51] Copyright from Elsevier, 2024. (c) Eight target gases detected by the proposed non-dispersive infrared architecture. Reproduced with permission.[52] Copyright from Springer Nature, 2020. (d) Optical nose for distinguishing meat products. Reproduced with permission.[53] Copyright from the American Chemical Society, 2021.

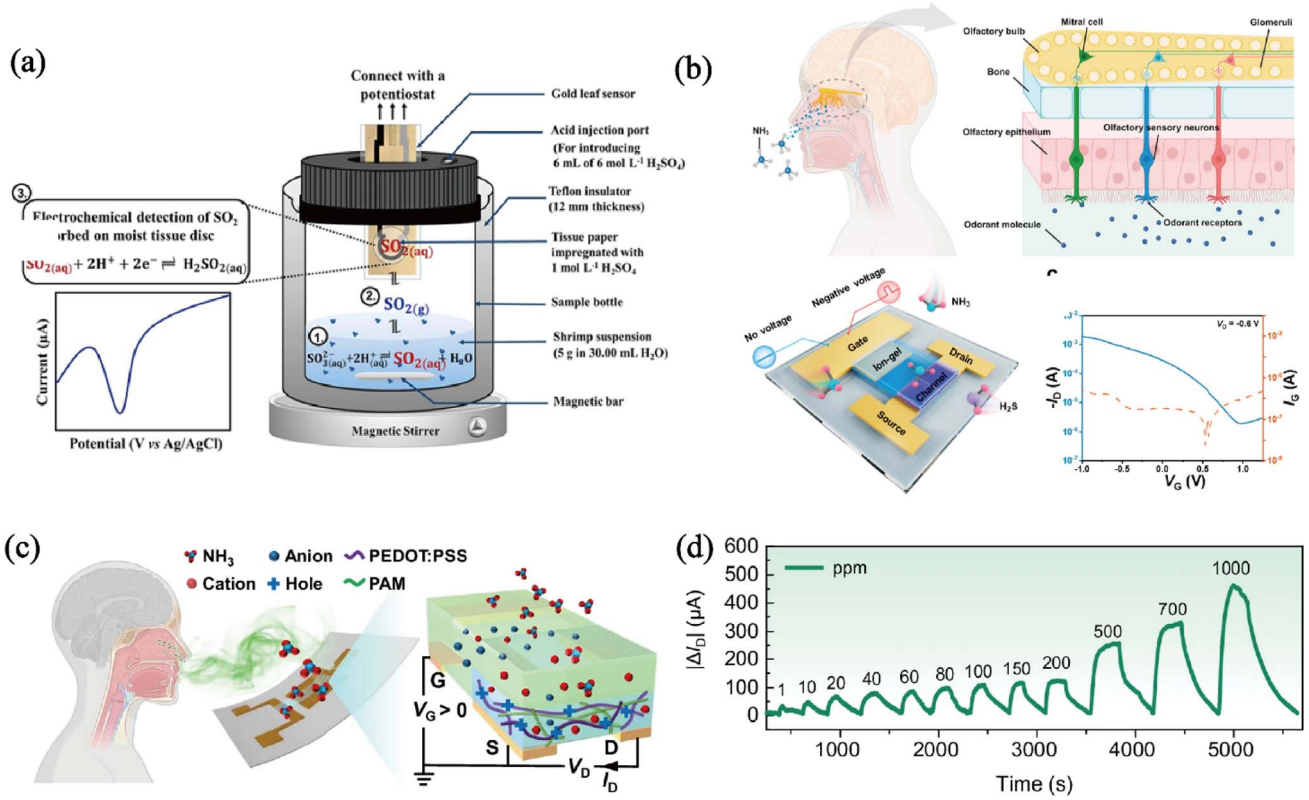

Fig. 6 (a) Schematic illustration of the electrochemical gas sensor. Reproduced with permission.[61] Copyright from Elsevier, 2023. (b) Schematics of the human olfactory system and an olfactory-inspired transistor configured for short-term and long-term potentiation states. Reproduced with permission.[62] Copyright from American Chemical Society, 2024. (c)–(d) A stretchable all-gel organic electrochemical transistor gas sensor with a PEDOT:PSS gel active layer. Reproduced with permission.[63] Copyright from Springer Nature, 2025.

advances the development of biomimetic artificial neuronal systems for chemosensory applications.[65,66] Another study presents a proof-of-concept for a bioengineered hybrid nasal construct that combines mechanically robust 3D bioprinted cartilage-like tissue with a biocompatible biosensing platform to replicate olfactory functionality. Utilizing multi-material 3D bioprinting with tunable chondrocyte-laden bioinks, the construct demonstrates enhanced cell viability and chondrocyte behavior. Integrated with an electrochemical biosensing system, the hybrid construct enables odor perception for specific airway disease biomarkers, explosives, and toxins, offering potential applications in functional bionic interfaces and humanoid cyborgs.[67] In another work, an organic electrochemical transistor was designed; the device simulates typical synaptic behavior to improve olfactory selectivity and obtain ppb-level responses. Meanwhile, the design of an organic electrochemical transistor (OECT) that simulates typical synaptic behavior is a significant advancement in the realm of

Table 3 Comparison of the predominant technological pathways for odor impression prediction

Technology	Mass spectrometry (MS)[75]	Electronic nose (E-nose)[76]	Structure–odor relationship (SOR)[77]
Principle	Measurement of mass-to-charge ratio of ionized molecules	Pattern recognition of global response from a sensor array	Computational modeling linking molecular structure to perceptual odor
Key advantages	High sensitivity & accuracy; unambiguous compound identification	Rapid, portable, real-time operation; cost-effective	No physical sample needed; predicts odor of novel molecules
Major limitations	Expensive, non-portable; requires skilled operation; poor real-time capability	Lower sensitivity/selectivity *vs.* MS; susceptible to environmental interference	Limited accuracy for complex mixtures; primarily theoretical
Suitable applications	Laboratory-based analysis; flavoromics; biomarker discovery	Food safety; environmental monitoring; medical diagnostics; quality control	Fragrance design; theoretical research; drug discovery
Cost & complexity	High	Low to medium	Low

bioinspired electronics and artificial intelligence, particularly for applications in olfactory sensing systems. This innovation not only pushes the boundaries of response in detecting trace amounts of substances (down to ppb levels) but also integrates the biological function of short-term and long-term memory, thereby enhancing the selectivity and intelligence of odor recognition.[68] Electrochemical gas sensors exhibit inherent memory functions, enabling their integration into bio-inspired systems. A recent study demonstrated this capability by implementing an artificial respiratory perception system on a single polymer substrate, combining a graphene oxide-based humidity sensor with an organic electrochemical transistor (OECT) functioning as an artificial synaptic device. The system demonstrates rapid response and high sensitivity, with the OECT exhibiting synaptic functionalities such as short- and long-term plasticity. It achieves parallel monitoring of over 100 respiratory states and distinguishes respiratory behaviors with a 5% difference, showcasing its potential for dynamic respiration monitoring and human health applications.[69] To further expand the capabilities of sensing technologies, researchers have developed advanced material platforms for enhanced sensitivity and stability. They present an olfactory biosensor for sensitive and stable hexanal detection, utilizing a novel receptor immobilization strategy based on ZIF-8@single-walled carbon nanotube (SWCNT) and nanosome-AuNPs/Prussian blue (PB). The ZIF-8@SWCNT dual support material provides abundant active sites for nanosome loading, while the co-electrodeposition of nanosome-AuNPs and PB enhances electrochemical signals and preserves receptor activity. The biosensor demonstrates exceptional performance, with a wide detection range (10^{-16}–10^{-9} M), an ultralow detection limit (10^{-16} M), and long-term stability (15 days), highlighting its potential for applications in food freshness monitoring.[70]

3.3 Molecular structure and olfaction

In recent years, the development of artificial intelligence technology has facilitated the creation of highly accurate data-driven models. Algorithms form the core foundation of artificial intelligence, governing the mechanisms of machine learning and data processing, while high-quality and diverse datasets are essential for model training and testing, ensuring robust performance. Odor prediction can be performed on molecular structure datasets using machine learning or deep learning algorithms.[71] As an odor dataset, molecular characterization datasets are the basic building blocks of taste and smell. In contrast to mass spectrometry data, electronic nose data, and electrochemical sensors, molecular characterization datasets respond explicitly to knowledge of molecular structure. For example, applying artificial intelligence technology can calculate 40 billion odorous compounds. This technology can quickly screen a large number of flavorful chemicals.

Molecular structures can be transformed into high-dimensional molecular characterization information by chemical software such as DRAGON, RDKit, and ADAPT. RDKit is an open-source Python software package for chemical information processing. The software package can transform the SMILES notation into molecular structure images (RGB), with carbon represented as black, oxygen as red, nitrogen as blue, sulfur as yellow, chlorine as green, and phosphorus as orange. It converts the molecular structures of compounds into 2D and 3D molecular data and subsequently employs machine learning techniques to analyze these compounds. For instance, a linear classification algorithm is used to predict the odor of molecules.[72] The method of olfactory weighted sum (OWSum) uses the structural features of the molecules as the data set and can directly analyze molecular odors. The SMILES strings of 1278 odorant molecules were set as the base dataset to train the algorithmic model. The model exhibited high precision (>99%) and high sensitivity (>99%) when predicting seven basic smells using an independent test dataset. In another work, researchers investigated the application of machine learning and data analytics to predict perceptual attributes of odorants, specifically the odorant characters (OC) of "sweet" and "musky," thus bridging a gap in olfactory research. A psychophysical dataset containing perceptual ratings from 55 subjects was analyzed to identify patterns in odor perception. Three machine learning approaches—random forest, gradient boosting, and support vector machines—were employed to model odor-characteristic relationships, revealing critical molecular descriptors governing odor perception. The impact of data quality on model performance was assessed by comparing semantic descriptors of odorants with their perceived attributes. The study presents a methodology for odor perception modeling, offering insights into untrained human perception and the influence of perceptual biases on model accuracy. The developed models and framework hold potential for predicting odor characters of novel odorants, advancing quantitative structure–property relation (QSPR) applications in olfaction research.[73] Similarly, researchers developed a winning random forest model during the DREAM Olfaction Prediction Challenge. This model accurately predicts both individual and population-level olfactory responses by integrating multi-scale perceptual data, denoising input signals, and leveraging a minimal set of highly discriminative molecular descriptors.

3.4 Comparative analysis of olfactory prediction technologies

A comprehensive understanding of the strengths and limitations of each technology is crucial for selecting the appropriate tool for specific olfactory prediction tasks. To provide a clear and systematic overview, Table 1 summarizes the core characteristics of the three predominant technological pathways discussed in this section. Furthermore, given the central role of the sensor array in e-nose performance, a detailed comparison of the most common sensor types is presented in Table 3.

As evidenced in Table 3, no single technology represents a universal solution. The choice is based on a trade-off between analytical precision (favoring MS), practical deployability (favoring E-nose), and theoretical prediction (favoring SOR modeling). MS serves as an offline reference technique, while E-noses are tailored for online, in-field applications. SOR models, while not directly used for device-based sensing, can guide the

design of new ligands and materials for sensors.[74] As for the electronic nose, the sensor selection for an e-nose defines its operational method. MOS sensors offer a low-cost entry, but with higher power needs and drift issues. Optical sensors provide superb performance but at a premium cost and size. Electrochemical sensors strike a balance for monitoring specific target analytes with low power consumption, making them ideal for portable/wearable devices.

4. Machine learning for olfactory prediction model

4.1 The paradigm shift to machine learning

The previous sections have laid the base for applying ML in olfaction. Section 2 provides the essential data foundation; the relationships within these datasets (*e.g.*, between molecular features and perceptual qualities) are often highly complex and nonlinear. Section 3 then reviewed the traditional technologies for capturing odor information and early prediction attempts. However, these data often face challenges with high-dimensional data, non-linear relationships, and feature selection. Machine learning technology, as a powerful paradigm, can overcome the inherent limitations of datasets. Meanwhile, ML algorithms, with their superior capacity for handling high-dimensional data and identifying complex patterns, are critically needed to construct accurate and robust olfactory prediction models. This is precisely where machine learning emerges as a transformative tool. This section will discuss how ML algorithms effectively integrate the databases with the sensing technologies to build powerful predictive models of olfactory perception.

4.2 Data acquisition from sensing devices and preprocessing

The efficacy of machine learning models in olfactory prediction is fundamentally dependent on the quality of the input data, which originates from the multi-channel sensor arrays of

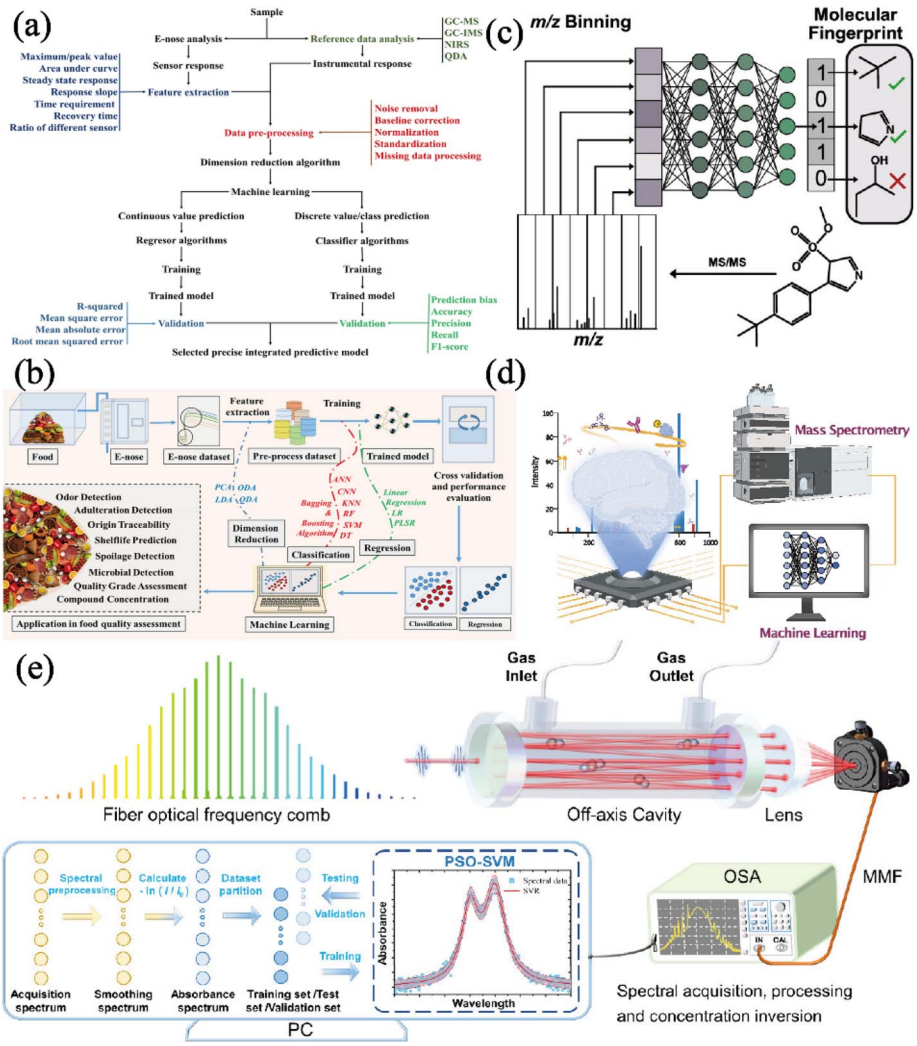

Fig. 7 (a) Preprocessing steps for olfactory data, along with a brief overview of the data processing workflow for ML algorithms. (b) The e-nose data preprocess. Reproduced with permission.[78] Copyright from Elsevier, 2025. (c) Mass to charge ratio and feed-forward neural network and (d) machine learning for mass spectrometry data. Reproduced with permission.[81] Copyright from the American Chemical Society, 2024. (e) Optical gas sensing data and SVM. Reproduced with permission.[82] Copyright from the American Chemical Society, 2024.

electronic noses (E-noses) as detailed in section 3. For instrument-collected data, the raw data is typically a multivariate time-series signal, capturing the dynamic response (*e.g.*, resistance change) of each sensor during baseline, odorant exposure, and recovery states. As shown in Fig. 7(a) and (b), the data features collected from e-nose systems include maximum/peak value, response slope, recovery time, ratio of different sensors, area under a curve, and steady-state response. Beyond electronic MOS, electrochemical gas sensors, optical gas sensors, and gas chromatography are also widely employed in odor analysis due to their distinct advantages in selectivity, sensitivity, and molecular specificity (as shown in Fig. 7(c)–(e)). Although the raw signal formats may differ—for instance, optical sensors typically measure absorption or fluorescence intensity over time, while GC produces chromatograms based on retention times—the subsequent feature extraction process shares common principles. Critically, all these technologies require the raw temporal signals to be converted into discriminative feature sets, including descriptors such as peak value, integral area, temporal derivatives, or normalized response ratios. These feature engineering steps form a common structured dataset that enables effective model training and cross-modal comparison, regardless of the original sensing technology.[78] Meanwhile, to transform complex and noisy temporal data into a suitable format for machine learning, the critical preprocessing method is employed. The relevant method involves reducing sensor drift, followed by feature extraction to distill key parameters from each sensor's response curve.[79] Subsequently, these data features undergo normalization (*e.g.*, *Z*-score standardization) to ensure all sensor channels contribute equally to the model, and are often subjected to dimensionality reduction techniques such as principal component analysis (PCA) to mitigate multicollinearity, visualize data structure, and improve model efficiency and performance.[80] This preprocessing method transforms raw sensor signals into refined, information-rich datasets, laying a crucial foundation for building robust olfactory prediction models.

4.3 Machine learning for olfaction analysis

In recent years, machine olfaction technologies have been undergoing a profound transformation that is driven by advances in sensor design, artificial intelligence algorithms, and diverse application scenarios (as shown in Fig. 8). To effectively process and interpret the complex data from advanced sensors, a variety of machine learning-based olfactory prediction methods have been developed. These include artificial neural networks, random forests, K nearest neighbors, support vector machines, extreme learning machines, gradient boosting decision trees, and decision trees.[85] These methods are suitable for analyzing datasets generated by various sensing devices (Table 4). Specifically, the choice of machine learning algorithm depends on the type of input data (class/binary or approximate numerical form), the kinds of available data (continuous or discrete), the data precision (complexity and dimensionality), the number of datasets, and the number of features in each dataset.[78] For example, classifying the complex aroma of coffee beans will address high-dimensional and continuous sensor data. To address this, researchers employed an array of TGS gas sensors coupled with a double-hidden-layer backpropagation neural network to classify Arabica coffee aromas according to roasting temperature. The results demonstrated excellent classification performance, achieving accuracies of 98.2% for light roasts, 98.4% for light-to-medium roasts, 97.8% for medium-to-dark roasts, and 95.9% for dark roasts. The findings demonstrate that the E-nose system, which combines TGS sensors and artificial neural networks, effectively detects and classifies coffee aromas according to roasting

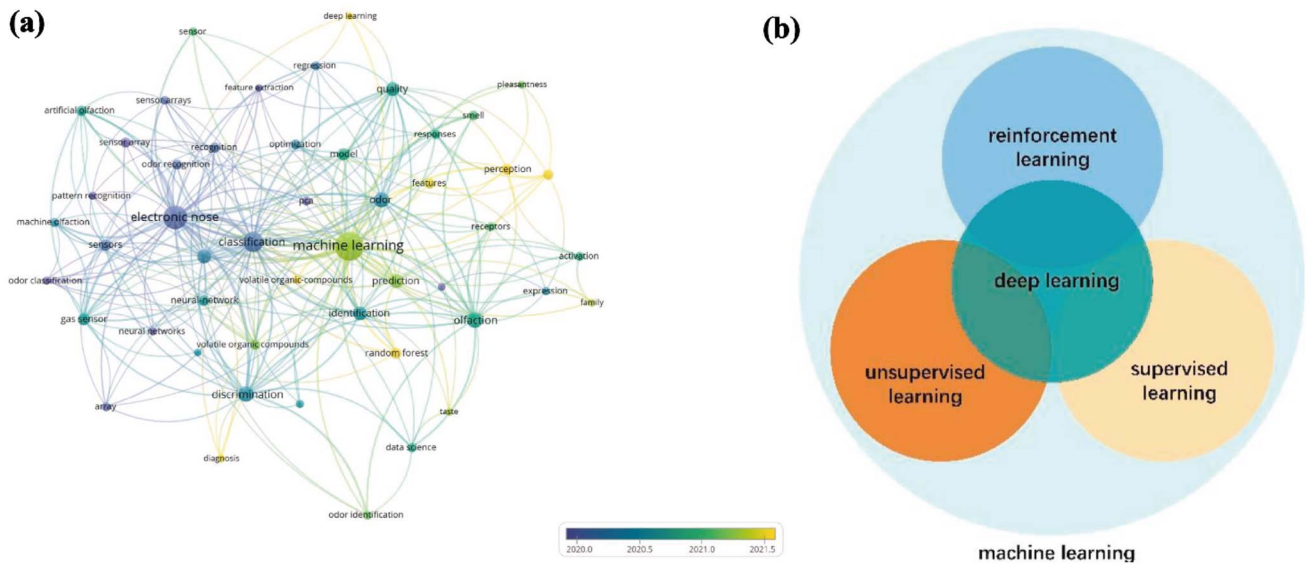

Fig. 8 (a) Evolution of machine learning in odor research (1977–2024). Reproduced with permission.[83] Copyright from Elsevier, 2024. (b) Diagram of machine learning. Reproduced with permission.[84] Copyright from Elsevier, 2023.

Table 4 Algorithm for sensing recognition

Algorithm	Sensor	Application	Focus	Ref.
ANN	MOS	Coffee	Classification of coffee types	86
ANN	MOS	VOCs	VOCs recognition	97
ANN	MOS	Maize	Maize quality monitoring	98
ANN	MOS	Beer	Assessment of aromas in beer	99
ANN	MOS	Coffee	Estimating the intensity of coffee	100
ANN	MOS	Sesame oil	Sesame oil quality assessment	101
ANN	MOS	Rice	Rice quality monitoring	102
ANN	FET	VOCs	VOCs recognition	103
ANN	MOS	Fruit juices	Quality monitoring of fruit juices	104
ANN	MOS	Oil-based plant	Quality monitoring	105
ANN	MOS	Fruit	Monitoring fruit ripeness	106
ANN	MOS	Beef	Beef quality monitoring	107
ANN	MOS	Rice	Monitoring pure and adulterated rice	108
ANN	MOS	Vinegar	Identify vinegar flavor	109
XGBoost-RF	MOS	VOCs	Predicting and classification of VOCs	87
KNN + LDA	MOS	Maize	Classification of moldy maize	88
SVM	Sensor array	Tea	Tea quality monitoring	90
SVM	NIR	Salmonid	Identification of off-flavor salmonids	110
SVM	MOS	Kiwifruit	Kiwifruit ripening monitoring	111
SVM	Near-infrared	Tea	Classification of tea	112
SVM	Colorimetric sensor array	Beef	Beef quality monitoring	113
SVM	MOS	Tea	Tea aroma monitoring	114
SVM	Visualization sensor	Tea	Evaluation of black tea fermentation	115
SVM	Visualization sensor	Oil	Classification of procymidone residues	116
ELM	MOS	Tea	Tea quality monitoring	91
GBDT	GC-MS	Fish meal	Monitoring freshness state	92
GBDT	MOS	Tea polyphenols	Tea quality monitoring	117
GBDT	MOS	Chinese baijiu	Recognition baijiu	118
GBDT	MOS	VOCs	VOCs recognition	119
DT	MOS	VOCs	Classification of explosives	94
RF		VOCs	Predicting VOCs	120
RF	MOS	Pecans	Classification of pecans	121
RF	MOS	Dried gingers	Classification of dried gingers	122
RF	MOS	Strawberry juices	Strawberry juice quality monitoring	123
RF	MOS	Peach	Peach maturation monitoring	124
RF	MOS	Peach	Peach growth cycle monitoring	125
RF	MOS	Orange	Orange quality monitoring	126
RF	MOS	Tea	Tea quality monitoring	127
RF	MOS	Kiwifruit	Ripeness of postharvest kiwifruit	128
RF	MOS	Milk	Milk quality monitoring	129
RF	MOS	Satsuma mandarins	Satsuma Mandarin quality monitoring	130
RF	Colorimetric sensor array	Tencha aroma	Assess tencha aroma	131
RF		VOCs	Predicting and classification of VOCs	132
MCNA	MOS	VOCs	VOCs recognition	96
BP + ELM	MOS	VOCs	Predicting and classification of VOCs	93

conditions.[86] The electronic nose (E-nose) is widely utilized for monitoring toxic gases, but conventional gas sensing relies on single estimators and limited training datasets, resulting in low classification and regression accuracy. To address these limitations, one study developed an E-nose system utilizing a gas sensor array and machine learning algorithms (XGBoost and random forest) for accurate gas type classification and concentration prediction. The XGBoost classifier achieves 96.0% accuracy, while the RF regressor attains an average R^2 score of 0.923 for six volatile organic compounds (VOCs). The system demonstrates high efficiency, with prediction times of 0.011 s for classification and 0.015 s for regression.[87] For the analysis of electronic nose array data, orthogonal partial least square-discriminant analysis (OPLS-DA) offers an advantage over random forest. OPLS-DA is a multivariate statistical method that integrates supervised pattern recognition and dimensionality reduction, widely applied in metabolomics, food science, and biomedicine. For instance, OPLS-DA successfully extracted characteristic biomarkers of moldy maize from complex VOCs, providing precise targets for subsequent sensor design and highlighting its practical value in food quality monitoring.[88] Optimization algorithms such as genetic algorithms (GA) offer advantages by efficiently performing high-dimensional feature selection to select the most informative sensor combinations, while simultaneously optimizing the hyperparameters of subsequent classification models. It enhances the overall system performance, interpretability, and robustness, while also reducing the risk of

overfitting.[89] Leveraging this advantage, the researchers analyzed time-dependent absorption spectroscopy data and employed a GA for optimal feature selection, ultimately developing a 15-unit sensor array. When integrated with a support vector machine (SVM) classifier, the array demonstrated exceptional performance, achieving 100% discrimination accuracy for varying concentrations of tea polyphenols (TPs) with a detection limit of 5 μM. Notably, the system reliably distinguished not only individual TPs at different concentrations but also complex mixtures. Beyond quantitative analysis, the method exhibited practical applicability, accurately differentiating eight green tea varieties (96.88% accuracy) and detecting adulteration in Biluochun tea samples with perfect (100%) classification performance.[90] In order to identify the quality of tea, Wang *et al.* used the extreme learning machine (ELM) method to improve the classification performance of the electronic nose: 98.20% for classification accuracy, 0.9871 for *F*1-score, and 0.9775 for kappa coefficient. In conclusion, this work indicated that ELM can effectively classify and detect tea based on E-nose measurements.[91] Gradient boosting decision tree is a powerful ensemble learning algorithm that achieves state-of-the-art performance on a wide range of tabular data problems. It operates by sequentially constructing decision trees, where each subsequent tree learns to correct the errors of the previous ensemble. This technique has also been successfully applied in food freshness assessments. For instance, in one study, GBDT was used to classify the freshness of 198 samples, and the model was constructed from the sensor array data and the freshness state. The GBDT model effectively discriminated fish meal samples into five freshness categories (super fresh, superior fresh, general fresh, corrupt, and completely corrupt) based on their VOCs. Furthermore, it demonstrated high predictive accuracy, achieving correlations of 0.90 with measured acid values and 0.97 with volatile base nitrogen (VBN) values from the E-nose data.[92] In addition to GBDT, other classical machine learning models, including support vector machines (SVM) and neural networks, have also exhibited remarkable performance. In another work, a model based on SVM and linear ridge classification (LRC) classified six types of gases with an accuracy value of 0.99. Meanwhile, the backpropagation (BP) neural network combined with the extreme learning machine (ELM) method performed well in predicting ethanol concentrations ($R^2 > 0.98$).[93] The integration of nanostructured sensor arrays with decision tree algorithms has shown significant potential for high-accuracy detection of hazardous chemicals. For instance, a nanowire sensor array combined with a decision tree algorithm successfully classified explosive types and estimated their concentrations, resulting in 93.75% accuracy and an average error rate below 4%.[94]

Despite the significant progress enabled by machine learning, several critical limitations persist in olfactory biosensing that define the forefront of current research. A primary constraint is the scarcity of large-scale, high-quality labeled datasets, as human sensory evaluation is inherently subjective, costly, and time-consuming, which inevitably restricts the complexity and generalizability of data-hungry deep-learning models. Moreover, the "black box" nature of many advanced algorithms poses significant challenges to interpretability,[95] hindering a clear understanding of odor–sensor interactions. For the data collection device, the E-nose systems typically suffer sensor drift, resulting in inaccurate measurement readings.[96] This limitation restricts their application in olfactory perception.

5. Conclusions and outlook

In this review, we summarize the recent advances in human olfaction perception and the corresponding olfactory prediction models. We have reviewed various olfactory simulation technologies, which demonstrated high accuracy and efficacy in detecting odor biomarkers. Several common methods can simulate human olfaction, including optical sensors, electrochemical sensors, metal-oxide semiconductors, gas chromatography-mass spectrometry (GC-MS), and computational odor prediction. These technologies can detect food ripeness, freshness, and storage time. The odor detection behavior, paired with a data-driven model, enables rapid and accurate detection of odor molecules. However, low selectivity and sensitivity are the main weaknesses of the sensor. Therefore, sensor arrays coupled with machine algorithms can simulate human olfaction by extracting most features. Machine learning algorithms performed well in high-dimensional data mining and data analysis.

Looking ahead, the limited number of sensors does not provide a complete picture of the odor flavor; thus, large sensing arrays that can collect more abundant olfactory signals are required. Collaborative interdisciplinary research involving machine learning and gas detection will also be instrumental in fostering next-generation odor-sensing techniques for olfactory perception. Simultaneously, there is a pressing need to advance explainable AI (XAI) techniques tailored for olfaction,[133] which can elucidate model decisions and potentially reveal novel sensor-odorant relationships. Furthermore, future efforts should focus on developing embedded artificial intelligence systems.[134] The systems should incorporate lightweight on-chip machine learning models for real-time edge analysis and explore multimodal fusion architectures that integrate complementary data from electronic noses, mass spectrometers, and even human sensory data. This approach will enable more comprehensive and powerful digital olfactory platforms.

Conflicts of interest

The authors declare no conflict of interest.

Data availability

No primary research results, software or code have been included, and no new data were generated or analysed as part of this review.

Acknowledgements

This work is financially supported by the China Tobacco Sichuan Industrial Co., Ltd (No. 202405500001).

References

1 L. C. Guo, H. R. Han, C. Y. Du, X. Ji, M. Dai, S. Dosta, Y. Zhou and C. Zhang, *Mater. Horiz.*, 2025, **12**, 1413–1439.
2 J. A. Gottfried, *Nat. Rev. Neurosci.*, 2010, **11**, 628–641.
3 H. W. Song, D. Moon, Y. Won, Y. K. Cha, J. Yoo, T. H. Park and J. H. Oh, *Sci. Adv.*, 2024, **10**, eadl2882.
4 L. L. Guo, J. Cheng, S. Lian, Q. Liu, Y. Lu, Y. Zheng, K. K. Zhu, M. H. Zhang, Y. L. Kong, C. Zhang, N. K. Rong, Y. M. Zhuang, G. X. Fang, J. J. Jiang, T. Y. Zhang, X. Han, Z. L. Liu, M. Xia, S. M. Liu, L. Zhang, S. D. Liberles, X. Yu, Y. F. Xu, F. Yang, Q. Li and J. P. Sun, *Nature*, 2023, **618**, 193.
5 C. Bushdid, M. O. Magnasco, L. B. Vosshall and A. Keller, *Science*, 2014, **343**, 1370–1372.
6 R. A. Potyrailo, S. Go, D. Sexton, X. Li, N. Alkadi, A. Kolmakov, B. Amm, R. St-Pierre, B. Scherer and M. Nayeri, *Nat. Electron.*, 2020, **3**, 280–289.
7 S. H. Sung, J. M. Suh, Y. J. Hwang, H. W. Jang, J. G. Park and S. C. Jun, *Nat. Commun.*, 2024, **15**, 1211.
8 H. W. Song, D. Moon, Y. Won, Y. K. Cha, J. Yoo, T. H. Park and J. H. Oh, *Sci. Adv.*, 2024, **10**, eadl2882.
9 C. Wang, Z. Chen, C. L. J. Chan, Z. a. Wan, W. Ye, W. Tang, Z. Ma, B. Ren, D. Zhang, Z. Song, Y. Ding, Z. Long, S. Poddar, W. Zhang, Z. Wan, F. Xue, S. Ma, Q. Zhou, G. Lu, K. Liu and Z. Fan, *Nat. Electron.*, 2024, **7**, 157–167.
10 J. Lötsch, D. Kringel and T. Hummel, *Chem. Senses*, 2019, **44**, 11–22.
11 R. S. Zhong, Z. L. Ji, S. Q. Wang and H. T. Chen, *Trends Food Sci. Technol.*, 2024, **153**, 104700.
12 H. Y. Zhao, S. M. Xu, S. N. Xie, W. L. Ye, J. Li, L. H. Wang, S. L. Cao, J. H. Cheng, X. A. Zeng and J. Ma, *Food Chem.*, 2025, **476**, 143392.
13 M. Schreurs, S. Piampongsant, M. Roncoroni, L. Cool, B. Herrera-Malaver, C. Vanderaa, F. A. Theßeling, Ł. Kreft, A. Botzki, P. Malcorps, L. Daenen, T. Wenseleers and K. J. Verstrepen, *Nat. Commun.*, 2024, **15**, 2368.
14 A. Keller, R. C. Gerkin, Y. Guan, A. Dhurandhar, G. Turu, B. Szalai, J. D. Mainland, Y. Ihara, C. W. Yu, R. Wolfinger, C. Vens, l. schietgat, K. De Grave, R. Norel, D. O. P. Consortium, G. Stolovitzky, G. A. Cecchi, L. B. Vosshall and p. meyer, *Science*, 2017, **355**, 820–826.
15 J. C. Rodriguez Gamboa, E. Eva Susana Albarracin, A. J. da Silva and T. A. E. Ferreira, *Data Brief*, 2019, **25**, 104202.
16 D. R. Wijaya, R. Sarno and E. Zulaika, *Data Brief*, 2018, **21**, 2414–2420.
17 R. Sarno, S. I. Sabilla, D. R. Wijaya, D. Sunaryono and C. Fatichah, *Data Brief*, 2020, **32**, 106139.
18 D. A. P. Gordillo, M. C. C. Castellanos, D. N. T. Barrera, J. A. E. Gomez, J. F. N. Sanchez and J. X. X. Leon-Medina, *Chemosensors*, 2022, **10**, 538.
19 J. W. Burns and D. M. Rogers, *J. Chem. Inf. Model.*, 2023, **63**, 7330–7337.
20 S. Kim, P. A. Thiessen, E. E. Bolton, J. Chen, G. Fu, A. Gindulyte, L. Han, J. He, S. He, B. A. Shoemaker, J. Wang, B. Yu, J. Zhang and S. H. Bryant, *Nucleic Acids Res.*, 2016, **44**, D1202–D1213.
21 J. Lozano, J. P. Santos, T. Arroyo, M. Aznar, J. M. Cabellos, M. Gil and M. D. Horrillo, *Sens. Actuators, B*, 2007, **127**, 267–276.
22 Z. Z. Li, M. Ha, D. Frank, P. McGilchrist and R. D. Warner, *Foods*, 2021, **10**, 3113.
23 K. Pastor, M. Ilic, J. Kojic, M. Acanski and D. Vujic, *Anal. Lett.*, 2022, **55**, 2220–2226.
24 W. Y. Zhu, F. Benkwitz and P. A. Kilmartin, *J. Agric. Food Chem.*, 2021, **69**, 3255–3265.
25 Y. F. Peng, C. Zheng, S. Guo, F. Q. Gao, X. X. Wang, Z. H. Du, F. Gao, F. Su, W. J. Zhang, X. L. Yu, G. Y. Liu, B. S. Liu, C. J. Wu, Y. Sun, Z. B. Yang, Z. L. Hao and X. M. Yu, *npj Science of Food*, 2023, **7**, 7.
26 C. Chen, J. Husny and S. Rabe, *Int. Dairy J.*, 2018, **77**, 19–28.
27 Z. Xing, D. Zogona, T. Wu, S. Pan and X. Xu, *Food Chem.*, 2023, **415**, 135650.
28 L. Liu, N. Na, J. Yu, W. Zhao, Z. Wang, Y. Zhu and C. Hu, *Advanced Science*, 2024, **11**, 2305639.
29 M. X. Xu, X. C. Hu, H. P. Zhang, T. Miao, L. Ma, J. Liang, Y. F. Zhu, H. Y. Zhu, Z. X. Cheng and X. H. Sun, *SENSORS*, 2025, **25**, 2633.
30 L. Chen, Q. Yu, C. Pan, Y. Song, H. Dong, X. Xie, Y. Li, J. Liu, D. Wang and X. Chen, *Talanta*, 2022, **246**, 123527.
31 Q. Ma, H. Li, S. Chu, Y. Liu, M. Liu, X. Fu, H. Li and J. Guo, *ACS Sustainable Chem. Eng.*, 2020, **8**, 5240–5250.
32 A. Afzal, N. Cioffi, L. Sabbatini and L. Torsi, *Sens. Actuators, B*, 2012, **171**, 25–42.
33 M. M. Hashemi, A. Nikfarjam, H. Hajghassem and N. Salehifar, *J. Phys. Chem. C*, 2019, **124**, 322–335.
34 W. Li, Y. Ren and Y. Guo, *Sens. Actuators, B*, 2020, **308**, 127658.
35 B. Yang, D. T. H. To, D. Sobolak, E. R. Mendoza and N. V. Myung, *Sens. Actuators, B*, 2024, **413**, 135741.
36 X. L. Wang, Y. W. Li, X. H. Jin, G. Sun, J. L. Cao and Y. Wang, *Sens. Actuators, B*, 2024, **403**, 135155.
37 S. Singh and S. Sharma, *Sens. Actuators, B*, 2022, **350**, 130798.
38 H. R. Yousefi, B. Hashemi, A. Mirzaei, H. Roshan and M. H. Sheikhi, *Mater. Sci. Semicond. Process.*, 2020, **117**, 105172.
39 Z. Q. Jiang, R. Zhao, B. Sun, G. D. Nie, H. Ji, J. Y. Lei and C. Wang, *Ceram. Int.*, 2016, **42**, 15881–15888.
40 L. Xu, R. Zheng, S. Liu, J. Song, J. Chen, B. Dong and H. Song, *Inorg. Chem.*, 2012, **51**, 7733–7740.
41 L. Wang, S. Ma, J. Li, A. Wu, D. Luo, T. Yang, P. Cao, N. Ma and Y. Cai, *Sens. Actuators, B*, 2021, **347**, 130642.
42 S. Zhu, L. Xu, S. Yang, X. Zhou, X. Chen, B. Dong, X. Bai, G. Lu and H. Song, *J. Colloid Interface Sci.*, 2020, **569**, 358–365.
43 L. Zhu, Y. Li and W. Zeng, *Ceram. Int.*, 2017, **43**, 14873–14879.
44 Q. Xie, Y. Ding, Q. Wang and P. Song, *Sens. Actuators, B*, 2024, **405**, 135338.

45 M. S. Lv, C. Li, Y. N. Li, X. F. Zhang, Z. P. Deng, X. L. Cheng, Y. M. Xu, L. H. Huo and S. Gao, *Sens. Actuators, B*, 2023, **375**, 132865.
46 M. Chen, X. Li, Y. Li, Y. Li, Z. Qin and Q. Wang, *Sens. Actuators, B*, 2024, **401**, 134951.
47 G. Wang, T. Chen, L. Guo, H. Wang, X. Wang, H. Zeng, Y. Feng, W. Zhao, Y. Wang, X. Liu, J. Wang and Y. Yang, *Sens. Actuators, B*, 2024, **413**, 135862.
48 X. Guo, Y. Ding, C. Liang, B. Du, C. Zhao, Y. Tan, Y. Shi, P. Zhang, X. Yang and Y. He, *Sens. Actuators, B*, 2022, **357**, 131424.
49 J. Bruce, K. Bosnick and E. K. Heidari, *Sens. Actuators, B*, 2022, **355**, 131316.
50 H. Kwon, O. Kamboj, A. Song, M. Alarcon-Correa, J. Remke, F. Moafian, B. Miksch, R. Goyal, D. Y. Kim, F. A. Hamprecht and P. Fischer, *Adv. Mater.*, 2024, **36**, 2402287.
51 Y. R. Wang, Z. L. Wang, Y. F. Gao, J. Yan and Y. L. Chen, *Sens. Actuators, B*, 2024, **409**, 135602.
52 X. C. Tan, H. Zhang, J. Y. Li, H. W. Wan, Q. S. Guo, H. B. Zhu, H. Liu and F. Yi, *Nat. Commun.*, 2020, **11**, 5245.
53 Z. Li and K. S. Suslick, *Acc. Chem. Res.*, 2021, **54**, 950–960.
54 A. A. Silva, L. A. M. Barea, D. H. Spadoti and C. A. De Francisco, *Opt. Eng.*, 2019, **58**, 1.
55 R. X. Dong, Z. Q. Shen, H. Z. Li, J. G. Cheng and Y. Y. Fu, *J. Mater. Chem. C*, 2024, **12**, 12692–12707.
56 M. N. Khannanov, A. B. Vankov, V. E. Kirpichev, L. V. Kulik and I. V. Kukushkin, *IEEE Sens. J.*, 2021, **21**, 24142–24148.
57 G. Antonacci, J. Goyvaerts, H. L. Zhao, B. Baumgartner, B. Lendl and R. Baets, *APL Photonics*, 2020, **5**, 081301.
58 C. Jiang, A. J. X. Guo, Y. Li, Y. Wang, J. Sun, Z. Chen, X. Chen and Q. Ma, *Chem. Eng. J.*, 2024, **484**, 149283.
59 G. Magna, E. Martinelli, R. Paolesse and C. Di Natale, *Sens. Actuators, B*, 2022, **373**, 132719.
60 M. Jaffar-Bandjee, T. Steinmann, G. Krijnen and J. Casas, *Proc. Natl. Acad. Sci. U. S. A.*, 2020, **117**, 28126–28133.
61 N. Jantawong, P. Prasertying, T. Wongpakdee, N. Khoonrueng, P. Aroonchat, N. Fukana, P. Wilairat, K. Uraisin and D. Nacapricha, *Sens. Actuators, B*, 2023, **385**, 133634.
62 Y. Yin, T. Sun, L. Wang, L. Li, P. Guo, X. Liu, L. Xiong, G. Zu and J. Huang, *ACS Sens.*, 2024, **9**, 4277–4285.
63 L. Lu, X. Liu, P. Gu, Z. Hu, X. Liang, Z. Deng, Z. Sun, X. Zhang, X. Yang, J. Yang, G. Zu and J. Huang, *Nat. Commun.*, 2025, **16**, 3831.
64 T. Elias Abi-Ramia Silva, F. Burisch and A. T. Güntner, *TrAC, Trends Anal. Chem.*, 2024, **177**, 117790.
65 H. H. Chouhdry, D. H. Lee, A. Bag and N.-E. Lee, *Nat. Commun.*, 2023, **14**, 132719.
66 Y. R. Lee, T. Tran Quang, B.-U. Hwang and N.-E. Lee, *Nat. Commun.*, 2020, **11**, 2753.
67 Y. A. Jodat, K. Kiaee, D. V. Jarquin, R. L. De la Garza Hernandez, T. Wang, S. Joshi, Z. Rezaei, B. A. G. de Melo, D. Ge, M. S. Mannoor and S. R. Shin, *Adv. Sci.*, 2020, **7**, 1901878.
68 Y. Deng, M. Zhao, Y. Ma, S. Liu, M. Liu, B. Shen, R. Li, H. Ding, H. Cheng, X. Sheng, W. Fu, Z. Li, M. Zhang and L. Yin, *Adv. Funct. Mater.*, 2023, **33**, 2370114.
69 Q.-L. Zhao, S.-W. Ma, H.-K. Zhang, M.-K. Rena, M.-Y. Zhang, J.-J. Yuan, Z.-L. Hou, L.-P. Fu, G.-P. He and M.-S. Cao, *Carbon*, 2024, **218**, 118765.
70 L. Jing, C. Yan Ping, H. Penglin, D. Ziyu, G. Yun, C. Songhe, M. Chao, X. Zhiping, X. Sun, Z. Yin, L. Ye and L. Yuan, *Food Chem.*, 2024, **442**, 138349.
71 J. Huizhuo, P. Dandan, S. Lijun, Z. Qingchuan, Y. Wenjing, K. Jianlei, Z. Min and Z. Yuyu, *Food Res. Int.*, 2025, **202**, 115707.
72 D. Schicker, S. Singh, J. Freiherr and A. T. T. Grasskamp, *J. Cheminf.*, 2023, **15**, 51.
73 R. Chacko, D. Jain, M. Patwardhan, A. Puri, S. Karande and B. Rai, *Sci. Rep.*, 2020, **10**, 17136.
74 H. Kaneshiro, M. Sato, A. Tanaka, S. Nakata, Y. Aihara, H. Kitoh-Nishioka, Y. Mori and S. Tanaka, *ACS Omega*, 2025, **10**, 39933–39945.
75 R. Epping and M. Koch, *Molecules*, 2023, **28**, 1598.
76 M. M. Ali, N. Hashim, S. Abd Aziz and O. Lasekan, *Trends Food Sci. Technol.*, 2020, **99**, 1–10.
77 M. Genva, T. K. Kemene, M. Deleu, L. Lins and M. L. Fauconnier, *Int. J. Mol. Sci.*, 2019, **20**, 3018.
78 S. S. Gite, M. Karmakar, S. Mokashi, C. G. Dalbhagat, V. Kambhampati, R. K. Raigar and R. M. Shukla, *Trends Food Sci. Technol.*, 2025, **159**, 104977.
79 J. Y. Guo, X. Li, X. L. Li, Z. Liang, J. X. Cao and X. L. Wei, *IEEE Trans. Instrum. Meas.*, 2024, **73**, 8.
80 W. Hu, L. Wan, Y. Jian, C. Ren, K. Jin, X. Su, X. Bai, H. Haick, M. Yao and W. Wu, *Adv. Mater. Technol.*, 2019, **4**, 1800488.
81 A. G. Beck, M. Muhoberac, C. E. Randolph, C. H. Beveridge, P. R. Wijewardhane, H. I. Kenttämaa and G. Chopra, *ACS Meas. Sci. Au*, 2024, **4**, 233–246.
82 G. Guan, A. Liu, X. Wu, C. Zheng, Z. Liu, K. Zheng, M. Pi, G. Yan, J. Zheng, Y. Wang and F. K. Tittel, *ACS Sens.*, 2024, **9**, 820–829.
83 R. Zhong, Z. Ji, S. Wang and H. Chen, *Trends Food Sci. Technol.*, 2024, **153**, 104700.
84 Y. Zhang, L. Deng, H. Zhu, W. Wang, Z. Ren, Q. Zhou, S. Lu, S. Sun, Z. Zhu, J. M. Gorriz and S. Wang, *Inf. Fusion*, 2023, **98**, 101859.
85 P. Jia, X. Li, M. Xu and L. Zhang, *Int. J. Bio-Inspired Comput.*, 2024, **23**, 16–27.
86 S. D. Astuti, I. R. Wicaksono, S. Soelistiono, P. Annissa, D. Permatasari, A. K. Yaqubi, Y. Susilo, C. D. Putra and A. Syahrom, *Sens. Biosens. Res.*, 2024, **43**, 100632.
87 W. Ni, T. Wang, Y. Wu, X. Chen, W. Cai, M. Zeng, J. Yang, N. Hu and Z. Yang, *IEEE Sens. J.*, 2024, **24**, 671–678.
88 H. Lin, Z. Chen, S. Y.-S. S. Adade, W. Yang and Q. Chen, *J. Agric. Food Chem.*, 2024, **72**, 11164–11173.
89 S. Parvaze, R. Kumar, J. N. Khan, N. Al-Ansari, S. Parvaze, D. K. Vishwakarma, A. Elbeltagi and A. Kuriqi, *Arch. Comput. Methods Eng.*, 2023, **30**, 4209–4244.
90 X. Yang, B. Zou, X. Zhang, J. Yang, Z. Bi, H. Huang and Y. Li, *Biosens. Bioelectron.*, 2024, **250**, 116056.
91 C. Wang, J. Yang and Q. Wu, *Meas. Control*, 2022, **55**, 746–756.

92 P. Li, J. Geng, H. C. Li and Z. Y. Niu, *Eur. Food Res. Technol.*, 2020, **246**, 1129–1140.
93 T. Wang, H. Ma, W. Jiang, H. Zhang, M. Zeng, J. Yang, X. Wang, K. Liu, R. Huang and Z. Yang, *Phys. Chem. Chem. Phys.*, 2021, **23**, 23933–23944.
94 J. Cho, X. Li, Z. Gu and P. U. Kurup, *IEEE Sens. J.*, 2012, **12**, 2384–2391.
95 C. Rudin, *Nat. Mach. Intell.*, 2019, **1**, 206–215.
96 J. Pan, A. Yang, D. Wang, J. Chu, F. Lei, X. Wang and M. Rong, *IEEE Trans. Instrum. Meas.*, 2022, **71**, 1–8.
97 T. C. Zhang, R. Q. Tan, W. F. Shen, D. W. Lv, J. Q. Yin, W. G. Chen, H. Y. Fu and W. J. Song, *Sens. Actuators, B*, 2023, **382**, 133555.
98 M. C. Leggieri, M. Mazzoni, S. Fodil, M. Moschini, T. Bertuzzi, A. Prandini and P. Battilani, *Food Control*, 2021, **123**.
99 C. G. Viejo, S. Fuentes, A. Godbole, B. Widdicombe and R. R. Unnithan, *Sens. Actuators, B*, 2020, **308**, 127688.
100 C. G. Viejo, E. Tongson and S. Fuentes, *Sensors*, 2021, **21**, 2016.
101 H. H. Ku, C. F. Lung and C. H. Chi, *Foods*, 2023, **12**, 4024.
102 A. Aznan, C. G. Viejo, A. Pang and S. Fuentes, *Foods*, 2022, **11**, 1181.
103 T. T. Wang, S. Q. Ma, A. F. Lv, F. J. Liu and X. B. Yin, *Sens. Actuators, B*, 2022, **363**, 131854.
104 M. Rasekh and H. Karami, *Int. J. Food Prop.*, 2021, **24**, 592–602.
105 M. Rasekh, H. Karami, A. D. Wilson and M. Gancarz, *Chemosensors*, 2021, **9**, 142.
106 P. Tyagi, R. Semwal, A. Sharma, U. S. Tiwary and P. Varadwaj, *J. Agric. Eng. Res.*, 2023, **54**, 1.
107 K. K. Pulluri and V. N. Kumar, *IEEE Sens. J.*, 2022, **22**, 15111–15122.
108 S. Vali Rasooli, K. Ali, K. Hamed, L. Jesus, T. Sylwester, D. Yousef and G. Marek, *Int. Agrophys.*, 2023, **37**, 235–244.
109 Y. Li, C. H. Fei, C. Q. Mao, D. Ji, J. W. Gong, Y. W. Qin, L. Y. Qu, W. Zhang, Z. H. Bian, L. L. Su and T. L. Lu, *Food Chem.*, 2022, **374**, 131658.
110 D. W. Sun, C. Q. Zhou, J. Hu, L. Li and H. B. Ye, *Food Chem.*, 2023, **408**, 135166.
111 A. Bakhshipour, *Food Sci. Nutr.*, 2023, **11**, 6116–6132.
112 L. Q. Li, S. M. Xie, J. M. Ning, Q. S. Chen and Z. Z. Zhang, *J. Sci. Food Agric.*, 2019, **99**, 1787–1794.
113 W. D. Xu, Y. C. He, J. H. Li, Y. Deng, J. W. Zhou, E. B. Xu, T. Ding, W. J. Wang and D. H. Liu, *Meat Sci.*, 2022, **194**, 108950.
114 T. An, Y. Li, X. Tian, S. X. Fan, D. D. Duan, C. J. Zhao, W. Q. Huang and C. W. Dong, *Sens. Actuators, B*, 2022, **371**, 132518.
115 T. An, W. Q. Huang, X. Tian, S. X. Fan, D. D. Duan, C. W. Dong, C. J. Zhao and G. L. Li, *Sens. Actuators, B*, 2022, **366**, 131994.
116 H. Jiang, M. X. Zhao and Q. S. Chen, *Food Chem.:X*, 2023, **19**, 100794.
117 B. H. Yang, L. Qi, M. X. Wang, S. Hussain, H. B. Wang, B. Wang and J. M. Ning, *Sensors*, 2020, **20**, 50.
118 M. L. Cao and X. Hu, *Electronics*, 2023, **12**, 79.
119 B. Wang, J. Y. Zhang, W. J. Li, Y. Y. Zhang, T. Wang, Q. Lu, H. Y. Sun, L. C. Huang, X. S. Liang, F. M. Liu, P. Sun and G. Y. Lu, *Sens. Actuators, B*, 2023, **377**, 133049.
120 X. Y. Zhang, K. Zhang, D. R. Lin, Y. Zhu, C. Chen, L. He, X. S. Guo, K. X. Chen, R. X. Wang, Z. Z. Liu, X. H. Wu, E. P. Long, K. Huang, Z. Q. He, X. Y. Liu and H. T. Lin, *GigaScience*, 2020, **9**, giaa011.
121 S. Jiang, J. Wang, Y. W. Wang and S. M. Cheng, *Sens. Actuators, B*, 2017, **242**, 511–521.
122 D. X. Yu, X. Zhang, S. Guo, H. Yan, J. M. Wang, J. Q. Zhou, J. Yang and J. A. Duan, *Food Chem.*, 2022, **396**, 133672.
123 S. S. Qiu, J. Wang and L. P. Gao, *J. Agric. Food Chem.*, 2014, **62**, 6426–6434.
124 H. G. J. Voss, R. A. Ayub and S. L. Stevan, *IEEE Sens. J.*, 2020, **20**, 11741–11750.
125 H. G. J. Voss, S. L. Stevan Jr and R. A. Ayub, *Comput. Electron. Agric.*, 2019, **163**, 104858.
126 S. Hazarika, R. Choudhury, B. Montazer, S. Medhi, M. P. Goswami and U. Sarma, *IEEE Trans. Instrum. Meas.*, 2020, **69**, 9010–9018.
127 M. Xu, J. Wang and L. Y. Zhu, *Food Chem.*, 2019, **289**, 482–489.
128 D. D. Du, J. Wang, B. Wang, L. Y. Zhu and X. Z. Hong, *Sensors*, 2019, **19**, 419.
129 F. L. Mu, Y. Gu, J. Zhang and L. Zhang, *Sensors*, 2020, **20**, 4238.
130 S. S. Qiu, J. Wang, C. Tang and D. D. Du, *J. Food Eng.*, 2015, **166**, 193–203.
131 S. S. Liu, Y. N. Rong, Q. S. Chen and Q. Ouyang, *Food Chem.*, 2024, **432**, 137190.
132 H. Y. Li, B. Panwar, G. S. Omenn and Y. F. Guan, *GigaScience*, 2017, **7**, gix127.
133 A. Barredo Arrieta, N. Díaz-Rodríguez, J. Del Ser, A. Bennetot, S. Tabik, A. Barbado, S. Garcia, S. Gil-Lopez, D. Molina, R. Benjamins, R. Chatila and F. Herrera, *Inf. Fusion*, 2020, **58**, 82–115.
134 X. Huang, H. Wang, S. Qin and S.-K. Tang, *Electronics*, 2025, **14**, 3468.